Biochimica et Biophysica Acta 1788 (2009) 600–607

Contents lists available at ScienceDirect

Biochimica et Biophysica Acta

journal homepage: www.elsevier.com/locate/bbamem

Melting of individual lipid components in binary lipid mixtures studied by FTIR spectroscopy, DSC and Monte Carlo simulations

M. Fidorra [a,b], T. Heimburg [a], H.M. Seeger [a,c,*]

[a] The Niels Bohr Institute, University of Copenhagen, Copenhagen, Denmark
[b] MEMPHYS-Center of Biomembrane Physics, Department of Physics, University of Southern Denmark, Odense, Denmark
[c] CNR-INFM National Research Center on 'nanoStructures and bioSystems at Surfaces S3', Via G. Campi 213/A, 41100 Modena, Italy

ARTICLE INFO

Article history:
Received 16 July 2008
Received in revised form 25 November 2008
Accepted 1 December 2008
Available online 14 December 2008

Keywords:
Domain formation
Phase separation
FTIR
MC simulation
DSC
Melting of individual lipid components

ABSTRACT

Monte Carlo (MC) simulations, Differential Scanning Calorimetry (DSC) and Fourier Transform InfraRed (FTIR) spectroscopy were used to study the melting behavior of individual lipid components in two-component membranes made of DMPC and DSPC. We employed Monte Carlo simulations based on parameters obtained from DSC profiles to simulate the melting of the different lipids as a function of temperature. The simulations show good agreement with the FTIR data recorded for deuterated and non-deuterated lipids, which demonstrates that the information on the differential melting of the individual components is already contained in the calorimetric profiles. In mixtures, both lipids melt over a wide temperature range. As expected, the lipid melting events of the lipid with the lower melting temperature occur on average at lower temperatures. The simulations also yield information on the lateral distribution of the lipids that is neither directly contained in the DSC nor in the FTIR data. In the phase coexistence region, liquid disordered domains are typically richer in the lower-melting-temperature lipid species.

1. Introduction

Biological membranes display a complex lipid composition. The reason for the large variety in lipid species is still not clear. It has been shown that for many different bacteria their lipid synthesis depends on physical parameters such as growth temperature or hydrostatic pressure [1–8]. It could further be demonstrated that the membranes of bacteria grown at higher temperatures contain more saturated fatty acid chains and that these chains tend to be longer [1–5,8]. Higher hydrostatic pressure induces an increased synthesis of unsaturated lipids [6,7], which has also been found for biological membranes from several deep-sea fish tissues [9]. This adaption has an influence on the physical behavior of a biological membrane, such as the melting transition behavior.

Melting transitions from a solid ordered (*so*; also called *gel*) to a liquid disordered (*ld*; also named *fluid*) phase can be found both in artificial and biological membranes [10,11]. In the latter case, they are typically found at temperatures slightly below body or growth temperature. In the presence of cholesterol, *liquid ordered* phases also develop [12]. When observing one component lipid membranes, one finds that a higher degree of saturation, or longer fatty acids, results in higher melting temperatures [13]. Therefore, one would expect that a change of the melting behavior of biological membranes depends on growth temperature or hydrostatic pressure. Indeed, this has been demonstrated for the prominent example of the inner membrane of Escherichia coli and other organisms [14].

The dependence of lipid synthesis on thermodynamic variables such as temperature or hydrostatic pressure has by some authors been called "homeoviscous adaption" [15,16]. The underlying idea was, that for a proper cell function, the membrane needs to provide a certain viscosity. Other authors have challenged this idea [17]. An alternative role of the adaption of lipid synthesis is to ensure a control of the heterogeneity of the lateral membrane structure [18]. This idea has obtained special attention within the discussion about "rafts", which are microdomains that are likely to exist in biological membranes [19]. Another important finding is that the elastic constants of membranes change significantly in transitions [20,21]. For this reason, geometrical changes in membranes are easier [22], permeabilities are increased [23] and pulse propagation becomes possible [24].

In the phase coexistence regime of model membranes consisting of two or three lipid species domains with sizes ranging from a few nanometers to several micrometers can be observed using a large variety of experimental techniques, such as Fluorescence Resonance Energy Transfer, Atomic Force Microscopy and Confocal Fluorescence Microscopy [25–29].

Since the early 1970s, the idea that domain formation processes can influence protein activity and function has been expressed [30,18]. In several publications, the existence of domains has been shown to provide a mechanism to control biochemical reaction cascades

* Corresponding author. CNR-INFM National Research Center on 'nanoStructures and bioSystems at Surfaces S3', Via G. Campi 213/A, 41100 Modena, Italy. Fax: +39 059 2055651.
E-mail address: heiko.seeger@unimore.it (H.M. Seeger).

0005-2736/$ – see front matter © 2008 Elsevier B.V. All rights reserved.
doi:10.1016/j.bbamem.2008.12.003

[31–34]. Evidence that lipid phase transitions and domain coexistence trigger enzyme activity has been found for various systems. For example, the enzyme phospholipase A_2, which hydrolyzes the *sn-2* bond of phospholipids, producing a free fatty acid and a lysolipid, displays the highest activity when the lipid membrane is in the lipid phase transition regime [35–37]. Changes in the opening times and probabilities of calcium channels reconstituted in POPE:POPC membranes of various ratios have been interpreted to be due to the coexistence of solid ordered and liquid disordered phases [39]. A further example is the protein kinase C (PKC) which modifies proteins by chemically adding phosphate groups. It has been discussed that lateral heterogeneities of the lipid membrane control the activation of this enzyme [40,41]. Other examples of a coupling between enzyme activity and the presence of specific lipids can be found, e.g. calcium ATPase [42].

The publications cited above are only a small selection, but they already show that it is important to study simultaneously domain formation and the fraction of the individual lipid species in the different domains. Individual lipid species will occur in varying amounts in the different domains or phases that form in a phase transition regime [43]. The work presented here concentrates on this for the case of a binary lipid mixture composed of *DMPC* and *DSPC*. These two phospholipids melt at 23.6 °C and 54.4 °C respectively [13]. In our study we used a deuterated *DMPC* derivate whose transition midpoint temperature lies at around 19–20 °C [44,45].

Various theoretical approaches have been used for the description of phase separation in lipid membranes. This includes ideal and regular solution theory, mean field, but also numerical approaches such as Monte Carlo (MC) simulations [43,46–48]. Ideal and regular solution theories permit the understanding of phase diagrams. In the ideal solution theory complete miscibility in the solid ordered and liquid disordered phase is assumed. Regular solution theory takes us a step further. It takes into account nearest-neighbor interactions that contribute to the overall enthalpy, however, entropic contributions to non-ideality are not considered. Both ideal and regular solution theories allow for the construction of phase diagrams. Phase diagrams are used to map the dependency of the phase behavior of lipid membranes upon, for example, temperature and lipid composition. The theoretically derived lever rule provides the possibility to determine the ratio of disordered and ordered lipids as a function of temperature and lipid composition of binary lipid mixtures and can also be applied to experimentally measured phase diagrams [43]. Ideal and regular solution theories are, however, based on simplifying assumptions. This does not only include an ideal mixing in both phases, but also the assumption of macroscopic phase separation under all conditions in the melting regime. In real systems, however, this is not the case since domains in lipid mixtures and in biological membranes are typically of finite size, much smaller than cell or vesicles size [49]. Furthermore, fluctuations are enhanced in the melting transition regime [20,50]. This is where MC simulations analyzing simple models of lipid chain melting obtain significance. They allow the consideration of interactions between different lipid species and varying chain state. The formation of lipid domains and fluctuations in state and position are included. Therefore, these simulations can clearly describe lipid membrane properties in the vicinity of lipid transitions, such as changes in membrane permeability [51], fluctuations in enthalpy [50] and diffusion processes [52,53].

In this study, we determined the amount of the individual lipid species in the different domains of binary *DMPC* and *DSPC* mixtures by means of MC simulations, and compared the results to experimental data measured by Fourier Transform InfraRed spectroscopy (FTIR).

FTIR is well suitable to the investigation of the melting behavior of lipid membranes. In these studies, the temperature dependence of various vibrational modes due to structural changes provides a versatile tool to measure phase transitions [54]. Articles have been published describing experiments in which FTIR was used to measure nanoscale domain size [55] and chain order parameters [56].

In our study, the hydrogen atoms of *DMPC* were replaced by deuterium atoms. Accordingly, the melting of the *DMPC* lipid chains could be separated from that of the *DSPC* lipid chain melting, as the CH_2 and CD_2 symmetric and asymmetric stretch vibrations differ in frequency due to the heavier deuterium atoms. This allowed us to compare the melting of individual components with MC simulation results which contain information on the disordered chain ratio of individual lipid components. MC simulations are also able to describe well experimental heat capacity profiles. The Monte Carlo simulations were used to relate the information from FTIR and the bulk melting behavior as determined by DSC.

In the following text, we show that DSC, MC and FTIR are a potent combination for investigating the melting behavior of lipid membranes. The fluctuation behavior of the different lipid species varies; this becomes important due to the enrichment of the individual lipids in various lipid domains. Therefore, the local membrane properties differ. We further provide another independent proof of the minimalistic model of Sugar et al. [48]. We also suggest a refined analysis of FTIR absorption spectra in order to follow the lipid membrane's phase transition.

2. Materials and methods

2.1. Sample preparation

The lipids 1,2-dimyristoyl-d54-sn-glycero-3-phosphocholine (*DMPC-d54*) and 1,2-distearoyl-sn-glycero-3-phosphocholine (*DSPC*) were purchased from Avanti Polar Lipids (Alabaster, USA). Samples were prepared from lipid stock solution. These were prepared in chloroform from lipid powder as delivered from the vendor without further purification. To prepare lipid samples in buffer, chloroform from the desired amount of lipid stock solution mixture was evaporated under a stream of nitrogen and the sample was kept under vacuum for several hours afterwards. After this procedure the dried lipid film was hydrated with preheated ultrapure water at a temperature of 60 °C, which is higher than the melting temperature of the higher-melting-temperature lipid component *DSPC* (54.4 °C, [13]) and kept stirring at this temperature for about 30 min. In calorimetric experiments a lipid concentration of 10 mM was used. The Fourier Transform Infrared spectroscopy measurements required concentrations of 65 mM. In order to facilitate lipid membrane hydration under these high concentrations the samples were subjected to several freeze–thaw cycles.

2.2. DSC experiments

Differential Scanning Calorimetry (DSC) experiments were performed on a VP-DSC (MicroCal, Northampton, MA, USA) with a scan rate of 15 °C/h (DMPC-d54:DSPC 50:50) or of 5 °C/h (DMPC-d54) in upscan direction. The samples were equilibrated at the starting temperature for 30 min.

2.3. Fourier Transform InfraRed spectroscopy experiments

Fourier Transform InfraRed (FTIR) spectroscopy experiments were performed on a Vertex70 (Bruker Optics, Bremen, Germany) equipped with a mercury-cadmium-telluride (MCT) detector. The spectrometer was flushed with nitrogen starting about 30 min before the experiments. Temperature control was carried out with the help of a purpose-built sample holder connected to a water bath (DC30-K20, ThermoHaake, Karlsruhe, Germany). The scan rate for the temperature ramp was set to 20 °C/h. The temperature in the sample corresponding to each temperature point set with the water bath was appointed in a reference scan. Background spectra were acquired at

each temperature point after lifting the sample compartment out of the beam path. We were interested in the IR absorption due to the symmetric and asymmetric stretch vibrational modes of the CH_2 and CD_2 groups of the lipid fatty acid chains.

Two methods to analyze the FTIR spectroscopy data were used. In a first approach, FTIR spectroscopy data was processed with a user-written plugin for the IGOR software package (WaveMetrics, Lake Oswego, OR, USA). The absorption peaks were fitted with a polynomial function from which the maxima positions were obtained.

For the second protocol, the peak area of the CH_2 or respectively of the CD_2 stretch vibrations was normalized to a value of $1\times cm^{-1}$. A reference spectrum was chosen, which was taken at a temperature below the melting transition regime. This spectrum was subtracted from all other spectra which were recorded at different temperatures. The peak area located at the positive axis of ordinates was then calculated and plotted as a function of temperature. This method was used by Heimburg et al. [58]. There was no difference in surveying both, symmetric and antisymmetric modes or the single ones. In the case of the CD_2 vibrations only the single modes were considered. In what follows, we shall call this method the *Difference Spectra method*.

2.4. Model

We have already applied an Ising-like model to the study of diffusion [52], fluctuation [50], and relaxation properties [57] of *DMPC:DSPC* lipid mixtures. In this paper, we used this model to describe FTIR measurements on *DMPC-d54:DSPC* mixtures and linked these to DSC measurements.

The model has been presented in detail elsewhere [52,48]. In short, the model is based on the assumption that the lipid chain states can be described by assigning either an ordered or disordered state to the fatty acid lipid chains. Lipid chains are arranged on a triangular lattice and only nearest-neighbor interactions are included. Lipid chains might change their states or their positions during the simulation. Formally, this corresponds to a 2-dimensional Ising model in a field. The model is evaluated with Monte Carlo (MC) simulations in which the free energy difference of an old and a trial configuration is sufficient for deciding upon the acceptance of a new configuration. The free energy of the system can be divided into a configuration dependent and an independent part. The configuration dependent contribution to the free energy of a given configuration equals [48]:

$$\Delta G = N_1^d(\Delta H_1 - T\Delta S_1) + N_2^d(\Delta H_2 - T\Delta S_2) + N_{11}^{od}\omega_{11}^{od} + N_{12}^{oo}\omega_{12}^{oo} + N_{12}^{od}\omega_{12}^{od} + N_{12}^{dd}\omega_{12}^{dd} + N_{12}^{do}\omega_{12}^{do} + N_{22}^{od}\omega_{22}^{od}, \quad (1)$$

where ΔH_i and ΔS_i are the enthalpy and respective entropy differences of the disordered and the ordered state of *DMPC* ($i=1$) and *DSPC* ($i=2$) lipid chains. ω_{ij}^{mn} are interaction parameters of unlike nearest-neighbors and N_{ij}^{mn} the corresponding number of the unlike nearest-neighbor contacts. m and n denote the state of a chain, which is either ordered (o) or disordered (d). Enthalpy, entropy and nearest-neighbor interaction parameters can be obtained from experimentally determined heat capacity profiles. Previously, we have determined the parameters needed for the *DMPC:DSPC* system [48,52]. In this paper, however, FTIR experiments were performed with *DMPC-d54* and *DSPC* mixtures. In the following, we made the assumption that the unlike species interaction parameters are the same in the *DMPC:DSPC* and in the *DMPC-d54:DSPC* mixtures. The heat capacity profile of the pure *DMPC-d54* was measured to obtain its enthalpy and entropy changes during the melting transition and the cooperativity parameter ω_{11}^{od} (*data not shown*). All values are listed in Table 1.

The simulations were performed on matrix sizes 60×60 (*DMPC-d54:DSPC* 100:0, 70:30, 60:40, 50:50, 40:60, 30:70 mol:mol), 100×100 (90:10, 80:20, 20:80, 10:90 mol:mol) and 350×350 (*DSPC*) [48]. The Monte Carlo cycles were defined by the three different possible Monte Carlo steps, namely state changes, exchanges of lipid position and lipid rotation. In one MC cycle each MC step was performed N times, where N is the total number of chains. The system was equilibrated for 5000 or, around the heat capacity maxima, for 10000 MC cycles. Simulations were conducted over 50000 or 100000MC cycles, respectively.

Table 1
Parameter values used in the Monte Carlo simulations

$T_{m,1}=19.7$ °C	$\omega_{11}^{od}=1267$ J/mol
$T_{m,2}=54.8$ °C	$\omega_{22}^{od}=1474$ J/mol
$\Delta H_1=14500$ J/mol	$\omega_{12}^{oo}=607$ J/mol
$\Delta S_1=49.5$ J/(mol °C)	$\omega_{12}^{dd}=251$ J/mol
$\Delta H_2=25370$ J/mol	$\omega_{12}^{od}=1548$ J/mol
$\Delta S_2=77.4$ J/(mol °C)	$\omega_{12}^{do}=1716$ J/mol

They were determined from experimentally determined heat capacity profiles [52]. All numbers are given per lipid chain. The indices *o* and *d* stand for ordered and disordered, respectively. *1* and *2* index *DMPC-d54* and *DSPC*.

3. Results

In this paper, we discuss melting processes in binary lipid mixtures. In doing so, we focus on the melting of the two individual components independently. Experimental FTIR and DSC measurements were accompanied by numerical simulations and an analysis of the corresponding phase diagram.

The evaluation of the model described in the Materials and methods section needs the determination of ten parameters. These include the melting enthalpies and entropies of the two lipids, and six unlike nearest-neighbor interactions. These parameters are known for *DMPC:DSPC* mixtures [48,52]. In the present studies, we used perdeuterated DMPC lipids. They display a melting temperature that is about 3.9 °C lower than that of *DMPC* (*data not shown*). Further, their melting peak is less cooperative. For this reason, we slightly adjusted the three parameters related to *DMPC-d54* melting, but kept all other parameters from the previous *DMPC:DSPC* simulations. To validate this, DSC measurements on an equimolar *DMPC-d54:DSPC* mixture were performed and they were compared to simulation results. We found that the simulated values describe the measured melting profile accurately (see Fig. 1). Therefore, we were convinced that it was feasible to continue using the model with the interaction parameters given in Table 1.

The aim of this paper was to compare the temperature dependence of the fractions of disordered chains from numerical simulations of *DMPC-d54* and *DSPC* lipids with the experimental analysis of the melting processes using FTIR spectroscopy.

In FTIR spectroscopy the absorption of infrared light due to molecular vibrations is studied. Different vibrational modes of the lipids contribute to the absorption spectrum. We particularly focused on CH_2 or CD_2 (in the case of the deuterated *DMPC* lipids) stretch vibrations of the fatty acid lipid chains. The shape of the absorption band is temperature dependent, as can be seen in the left panel of Fig. t2. Example spectra of the symmetric and asymmetric CH_2 vibrational spectra are given for different temperatures of a *DMPC-d54:DSPC 40:60* mixture. Deuterium atoms are heavier than hydrogen atoms; this leads to a shift of the CD_2 stretch vibrations to lower wavenumbers, and allows us to distinguish the two different lipid species in a binary lipid mixture.

3.1. Comparison of FTIR results and Monte Carlo simulations

In an investigation of structural changes in cytochrome *c*, Heimburg and Marsh [58] analyzed difference spectra. This is a very common method in time resolved infrared spectroscopy. The assumption in the above study was that spectral changes are mostly due to changes in the fractions of two well-defined molecular states. However, in order to study the degree of melting in lipid membranes, the temperature shift of the CH stretching bands is often used. Since

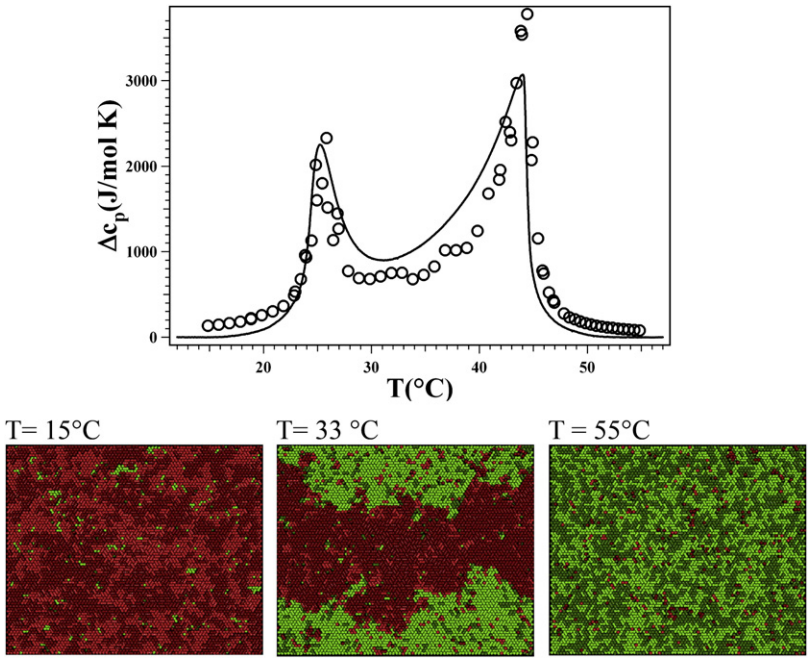

Fig. 1. Enthalpy and entropy changes and cooperativity parameters of the one component *DMPC-d54* and *DSPC* lipid membranes were determined from heat capacity profiles. The remaining four unlike species nearest-neighbor interaction parameters of *DMPC-d54:DSPC* mixtures were assumed to equal the ones of a *DMPC:DSPC* system [52]. Simulating an equimolar mixture of *DMPC-d54* and *DSPC* gives a melting profile (*open circles*) which describes well the heat capacity profile measured (*solid curve*). Below three representative snapshots from simulations of the same mixture with a matrix size of 80×80 lipid chains are shown. The red and green colors represent ordered or disordered lipid chains, respectively. The lighter colors correspond to the *DMPC-d54* lipid chains and the darker ones to the *DSPC* lipid chains. The snapshots were taken at three different temperatures. At a temperature of 15 °C the membrane is in the *solid ordered* phase while at a temperature of 55 °C it is in the *liquid disordered* phase. In both cases lipids do not mix ideally, but lateral heterogeneities are present. Two macroscopic phases are present at a temperature of 33 °C.

we suspected that the CH bands are a superposition of ordered and disordered lipid spectra, we decided instead to study difference spectra. We will show below that this is a much better method of analyzing lipid melting in FTIR than studying shifts in band positions.

Difference spectra were calculated for all spectra measured at various temperatures. In the left panel of Fig. 2, spectra of the CH_2 stretch vibrations are shown as a function of the temperature of a *DMPC-d54:DSPC 40:60* mixture. The reference spectrum was taken at a temperature of −7.6 °C. Representative examples of the difference spectra are displayed in the right panel of Fig. 2. To follow the melting transition, the change in difference spectra peak area of the CH_2 or the CD_2 vibrational modes (symmetric, asymmetric or both) can be monitored. Our experiments showed that there is no difference between these three approaches (*data not shown*).

The temperature dependent evolutions of the difference spectra peak areas are given in Fig. 3 as solid curves for four different *DMPC-*

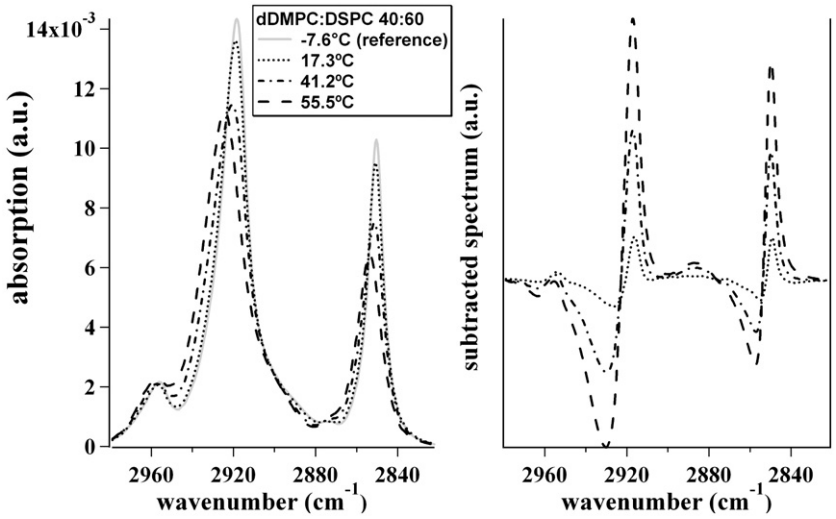

Fig. 2. The IR absorption spectrum contains different absorption maxima originating from varying vibrations. In the *left* panel the asymmetric and the symmetric CH_2 stretch vibrations as measured in a sample of *DMPC-d54:DSPC 40:60* at different temperatures are displayed. The absorption maxima of these are temperature dependent and lie at around 2852 cm^{-1} (symmetric) and at 2925 cm^{-1} (asymmetric). The asymmetric and symmetric CD_2 stretch vibrations are shifted to lower wavenumbers due to the heavier deuterium atoms (*data not shown*). In previous studies from other labs the melting processes were investigated following the temperature dependence of the absorption maxima. In this study, however, the melting process was also studied by defining a reference spectra (here taken at a temperature of −7.6 °C) and subtracting this one from all other spectra where in each case the area was normalized to 1×cm^{-1} (*Difference Spectra method*). Example results of the difference spectra of the left panel are displayed in the *right* panel. As a measure of the progress of the melting process the area of one of the peaks was taken.

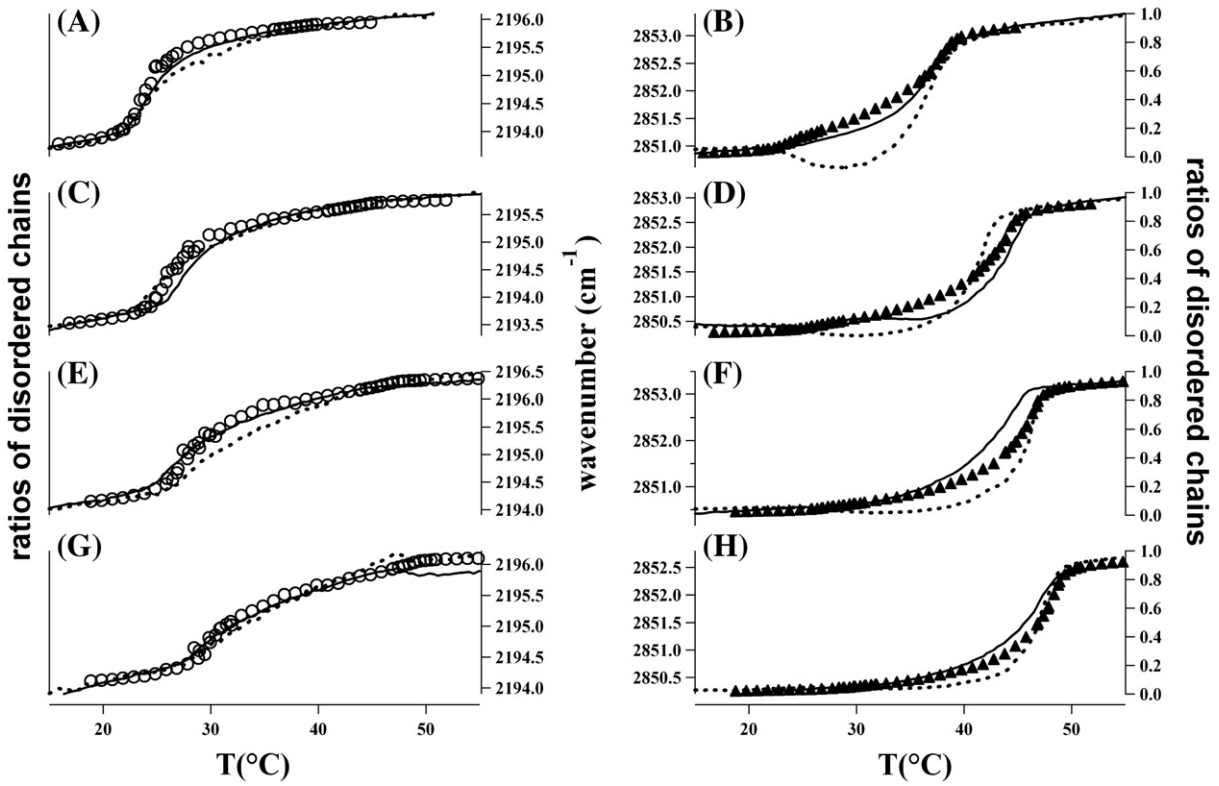

Fig. 3. The FTIR results are compared with the Monte Carlo simulations. The data on four different *DMPC-d54:DSPC* ratios *70:30* (A, B), *50:50* (C, D), *40:60* (E, F) and *30:70* (G, H) are displayed. In each panel the disordered chain ratios obtained from the simulations (open circles (*DMPC-d54*) and solid triangles (*DSPC*)) are compared with the changes of the peak area (solid curves) and the evolution of the position of the absorption maximum (dashed curves). In the latter case the antisymmetric CD_2 (*DMPC-d54*) and the symmetric CH_2 stretch vibrations were followed. The panels on the left side depict the melting process of the deuterated *DMPC-d54* lipids (A, C, E, G) and the right ones the *DSPC* lipid melting (B, D, F, H). The Monte Carlo simulations allow to combine both the FTIR and the calorimetric results. They provide a mean to relate the macroscopic with the microscopic behavior of the binary lipid membrane melting.

d54:DSPC mixtures: (A,B) *70:30*, (C,D) *50:50*, (E,F) *40:60* and (G,H) *30:70*. The panels on the left side show the results related to the deuterated *DMPC-d54* lipids (A,C,E,G) and those on the right give the data belonging to the *DSPC* lipids (B,D,F,H). The data is also compared to simulation results of the fraction of disordered lipid chains for each of the individual species. In Fig. 3 these are given as open circles

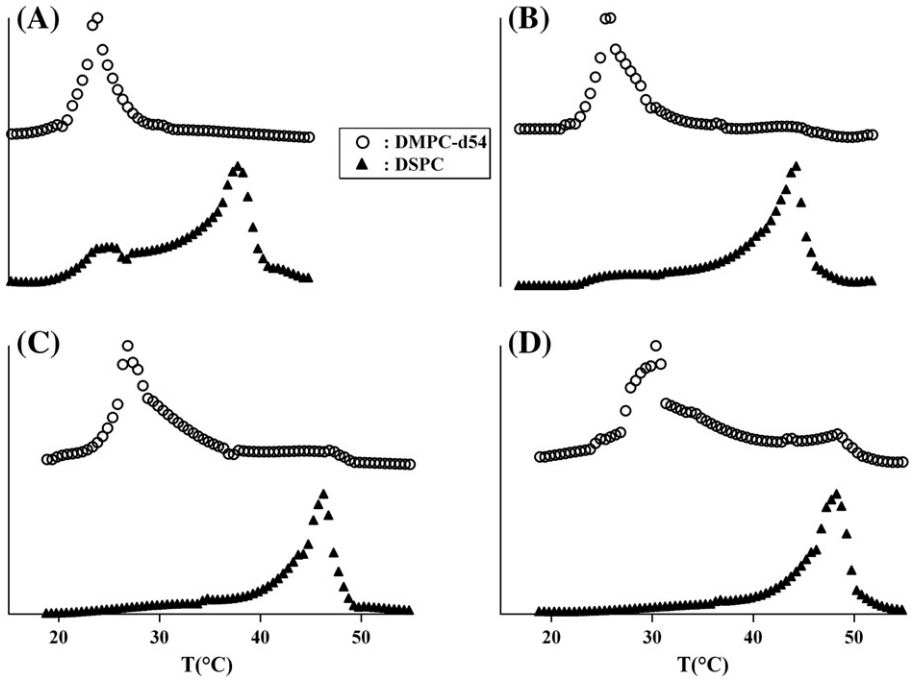

Fig. 4. The derivatives of the curves of the fraction of disordered *DMPC-d54* and *DSPC* lipid chains as shown in Fig. 3 are displayed in this figure. In detail these are the mixtures *70:30* (A), *50:50* (B), *40:60* (C) and *30:70* (D). The derivatives belonging to *DMPC-d54* are indicated by open circles, while the ones of *DSPC* by solid triangles. A maximum in the derivative means that at this temperature macroscopic and local fluctuations are enhanced.

(*DMPC-d54*) or solid triangles (*DSPC*). In all cases, we found an increase of the difference spectrum area with higher temperatures. There is good agreement between the simulated and measured values. The deviations between simulated and measured data are smaller in the cases of the *DMPC-d54* lipids. This might be due to the fact that the determination of the required model parameters is not perfect.

As already mentioned above, melting processes of lipid membranes investigated by FTIR were previously analyzed by monitoring the temperature dependence of the position of the absorption maximum of either the symmetric or asymmetric stretch vibrations of CH_2 and DH_2. We analyzed the temperature-dependence of the absorption maxima for several *DMPC-d54:DSPC* mixtures as previously done by Leidy et al. [26]. The results obtained are indicated by the dashed curves in Fig. 3.

We confirmed the results of Leidy et al. [26]. There are instances when the positions of the maxima of the symmetric stretch vibrations of the *DSPC* lipids do not increase with higher temperatures, but that for certain lipid mixture fractions they decrease, approach a minimum, and then start to increase again. In these cases, the minimum wavenumber is lower than the wavenumbers determined at lower temperatures. This behavior is contrary to the evolution of the difference spectra peak area and the MC simulation results. These findings are discussed below.

It is well known that macroscopic, but also local fluctuations of various membrane properties are enhanced in the vicinity of lipid membrane melting transitions. Fluctuations in area, volume or enthalpy are all mutually proportional [20,21]. The fluctuation–dissipation theorem [59] relates these to isothermal area or volume compressibilities, or to the heat capacity, which are all at a maximum when fluctuations are strongest [20,50]. The derivatives of the curves from Fig. 3 contain information on the strength of these fluctuations as well. In Fig. 4 these derivatives are shown for the simulated data. The curves given independently for the two lipids can be considered as melting profiles of the individual species. The higher the value of the derivative, the stronger the fluctuations are. The derivatives in the left panels of Fig. 4, which correspond to the *DMPC-d54* lipids (*open circles*), have maxima at lower temperatures than the derivatives belonging to the *DSPC* lipids (*solid triangles*). This supports the view that, at lower temperatures, mainly *DMPC-d54* lipids melt and at higher ones the *DSPC* lipids. The temperatures, however, depend on the ratio between the two lipid species. The more *DMPC-d54* is present, the lower the temperatures at which both species display their enhanced fluctuation behavior. In this context, it should be noted that the component which is in the minority always displays two maxima, one local and one global. The local maximum is found at a temperature at which the other component displays its strongest fluctuations. At an equimolar ratio of *DMPC-d54:DSPC* this is true for both components. The melting events of the individual lipid components occur over a broad temperature regime.

4. Discussion

In this paper we have presented a combined numerical and experimental study exploring melting processes in binary lipid mixtures. In detail, we focused on the melting of the individual lipid components *DMPC-d54* and *DSPC*. Monte Carlo simulations linked FTIR and DSC measurements to each other and thus MC simulations proved once more to be a useful and powerful tool in exploring melting transitions in lipid membranes.

4.1. FTIR measurements

FTIR allowed us to measure the absorption spectra of lipid suspensions consisting of MLVs with varying *DMPC-d54* and *DSPC* ratios as a function of temperature. In particular we probed the CH_2 and CD_2 vibrational modes of the lipid fatty acid chains. The deuterium is heavier than the hydrogen atom which is why the symmetric and asymmetric bands of the CH_2 and CD_2 stretch vibrations display absorptions at different wavenumbers. This made it possible to distinguish the *DMPC-d54* and *DSPC* lipids.

We applied two different methods to analyze the measured absorption spectra. One was based on monitoring the temperature-dependence of absorption maxima corresponding to the CH_2 and CD_2 stretch vibrations. The other one was based on following changes in the peak area of difference spectra (*Difference Spectra method*).

Using the first method we found, in accordance with Leidy et al. [26], that for some mixtures the absorption maximum of the CH_2 stretch vibrations of the *DSPC* lipids shifted towards smaller wavenumbers with increasing temperature. This was when the *DMPC-d54* started to display stronger fluctuations (see the right panels of Fig. 3). With further increasing temperature wavenumbers started to rise again. This behavior has been interpreted to be due to a higher ordering of *DSPC* [38]. There is, however, no further supporting evidence that this is indeed the case. Actually, it should be considered that this would mean a higher ordering than the one found at lower temperature. In contrast, this behavior disagrees with our findings from the second, the Difference Spectra method, and as well as with the Monte Carlo simulations, which we discuss in the next paragraph. Therefore, it seems reasonable that the Difference Spectra method yields results which describe the melting process correctly and monitoring band shifts can only lead to incorrect results. In addition, it should be stated that attributing the degree of melting to a CH-stretching band shift lacks a theoretical justification and is probably just wrong.

4.2. Monte Carlo simulations

We compared the corresponding experimental results to the temperature-dependent ratio of disordered chains of the individual lipid species using MC simulations of a simple model (see Fig. 3). These numerical simulations were based on a Doniach model of the lipid chain melting process assuming one ordered and one disordered lipid chain state [61]. Only nearest-neighbor interactions were considered and the lipid chains were arranged on a triangular lattice. Even though it is a minimalist model which only implicitly includes the fact that lipid chains may reflect different degrees of disorder, and further does not consider the loss in lattice order, the calculated fraction of disordered lipid chains of the individual lipid species describes well the experimental data obtained using the *Difference Spectra method*.

This model has previously been shown to describe heat capacity profiles as measured with DSC [48,52,50]. Ten unique parameters, which were obtained from experimental heat capacity profiles, are needed. Entropy and enthalpy changes, the corresponding cooperativity parameters, follow directly from the heat capacity curves of the one lipid component systems. The missing four parameters have to be found by fitting the heat capacity profiles of the binary mixtures. In our case we have taken the remaining four parameters from the *DMPC:DSPC* system [52]. This proved to be valid, but small deviations due to this assumption cannot be excluded completely.

Heat capacity profiles contain macroscopic information on the melting behavior, such as changes in enthalpy and entropy. However, DSC does not allow us to determine the microscopic behavior, such as domain formation and local fluctuations. Nor does it allow us to investigate the melting of the individual components. FTIR, however, provides a means of studying the melting of individual lipid species and of observing the microscopic details, but lacks the possibility to probe macroscopic properties such as domain formation and component demixing. The model underlying the MC simulations describes heat capacity profiles and predicts the findings from FTIR accurately. Therefore, the MC simulations link the information of the two experimental techniques.

4.3. The melting process

Considering one-lipid-component systems, it is well known that *DMPC-d54* lipid membranes melt at lower temperatures than *DSPC* lipid membranes. This is also true for their behavior in binary mixtures as it becomes evident from the experimental and the simulated results and their corresponding derivatives (Fig. 4). It is worthy of comment that fluctuations assigned to the individual lipid components are enhanced at distinct temperature regimes, but both lipid species melt over the whole temperature regime of the transition. The minor lipid component may even show two temperature regimes with maxima in fluctuations.

The temperatures at which the fluctuations of the two components are strongest, as obtained from the simulations and the experiments, agree well (Fig. 5). The numerical simulations allowed us to calculate the fluctuations of the enthalpy of the individual components and the disordered chain fractions simultaneously. Therefore, we were able to compare the temperatures at which the fluctuations are at maximum with the temperatures determined from the derivatives of the disordered chain fractions; these temperatures are equal. In Fig. 1, the heat capacity profile of the equimolar mixture displays two maxima. The maximum at lower temperature corresponds to the enhancement in fluctuations of the *DMPC-d54* lipids, and the one at higher temperature to that of the *DSPC* lipids. There are cases when the heat capacity profile displays only one maximum, even though one can determine two temperatures using the evolution of the individual lipid disordered chain ratios. This is because DSC describes the bulk behavior, and single events may not be detectable since they show only a small contribution to the overall melting.

4.4. The phase diagram

Phase diagrams are generally constructed to easily access the phase behavior of complex lipid mixtures [43]. In our case a phase diagram depending on lipid composition and temperature was constructed. A phenomenological method to construct these involves aligning tangents on the lower and upper temperature limits of heat capacity profiles. This results in a solidus and a liquidus line as indicated by the grey curves in Fig. 5. If the lipid composition and temperature are known, the physical state of the membrane can be determined. Below the solidus line the lipid membrane is in the *solid ordered* phase, while above the liquidus line it is in the *liquid disordered* phase. Moreover, the liquidus and the solidus lines define the phase coexistence regime. The three snapshots in Fig. 1 provide a visual impression of this. At temperatures of 15 °C and 55 °C, the lipid membrane is in either the *solid ordered* or *liquid disordered* phase, respectively. It should, however, be mentioned that the mixing of the two lipids is not ideal in either of the two cases; the individual lipid species cluster. At a temperature of 33 °C, the two phases coexist and a macroscopic phase separation is present. In an earlier publication, we were able to show that one needs to distinguish between microscopic and macroscopic phase separation, and local fluctuations in chain state enter the physical picture. These fluctuations are enhanced at domain or phase boundaries. Small domains are also subject to strong fluctuations [50]. When analyzing phase diagrams, one should note that these physical effects are in general not considered in their interpretation. In addition, it has been pointed out that the construction of a phase diagram is, strictly speaking, only valid if the transition is of first-order [60]. The transition of binary lipid mixtures of *DMPC* and *DSPC* has been claimed to be of second order and therefore the interpretation of the phase diagram has to be regarded with caution [49]. The interpretation with the MC simulations does not create these ambiguities because it does not assign phases as such.

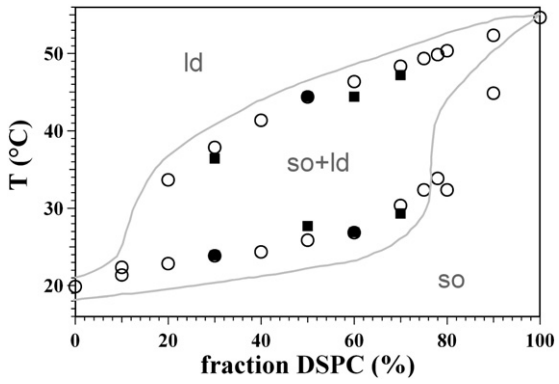

Fig. 5. Phase diagrams allow to obtain an understanding of the phase behavior of lipid mixtures in dependence of lipid ratios, temperature, pH or other outer parameters. In this study binary lipid mixtures were used to study melting transitions in dependence of temperature. Therefore, a phase diagram with the fraction of *DSPC* lipids as the abscissa and temperature as the ordinate was constructed. The grey lines represent the lower and upper temperature limits of the melting process as determined from heat capacity profiles simulated using the tangent method. Further the peak positions of the derivatives of the disordered chain fractions simulated (open circles) and of the experimentally determined area changes (filled squares) were analyzed. The simulated peaks determined from the derivatives agree with the maxima of the heat capacity profiles (*data not shown*).

4.5. Biological relevance

The model of a biological membrane by Singer and Nicolson considers the biological membrane to be mainly homogeneous [62], even though the possibility of protein aggregation was already included. In recent years this view has changed. A heterogeneous membrane model has modified this earlier picture [63,64]. Different kinds of heterogeneities can be present in biological membranes, such as protein aggregates or lipid domains. Even if a membrane was completely in the *liquid disordered* phase, lipids might not mix ideally and a heterogeneity exists as seen in Fig. 1 and as already discussed elsewhere [50]. This statement also holds for membranes in the *liquid ordered* phase [65]. The role of lipid membrane heterogeneities has been discussed exhaustively in the literature [18,31,34–37,39–42,66]. It has not only been pointed out that the coexistence of *solid ordered* and *liquid disordered* phases may be important [35–37,39,40], but also the enrichment of individual lipid species in certain regions of the lipid membrane [38,41,66,42].

The melting of individual components cannot be detected from the bulk melting in a calorimeter. However, most of the publications cited here deduce phase separation of natural membranes from calorimetric results.

In this context, not only the various lipid membrane phases such as the liquid disordered or solid ordered phases have to be considered, but also the possibility of enrichment of certain lipid species in particular lipid domains. The existence of heterogeneities depends on the details of the thermodynamical properties and the lipid interactions. As seen in this study, they melt over a broad temperature regime with temperatures at which they display strong fluctuations in more complex lipid mixtures. Since different lipids are enriched in different domains, the fluctuations will also have different strengths at different locations in the lipid matrix. This is especially interesting, since it is known that the fluctuations are related to elastic constants [20,21]. It implies that, at different temperatures, different regions of the membrane are soft and flexible.

A possible reason for the large variety in lipid species in biological membranes might be to ensure a required lipid membrane heterogeneity and the local degree of fluctuations that expresses itself in the local elastic constants.

Acknowledgements

M. Fidorra was funded by BioNet and the Villum Kann Rasmussen Foundation. We thank M. Ruis and B. Murray for their critical reading of the manuscript.

References

[1] A.G. Marr, J.L. Ingraham, Effect of temperature on the compositions of fatty acids in *Escherichia Coli*, J. Bacteriol. 84 (1962) 1260–1267.
[2] P.V. Johnston, B.I. Roots, Brain lipid fatty acids and temperature acclimation, Comp. Biochem. Physiol. 11 (1964) 303–309.
[3] M. Kleinschmidt, V.A. McMahon, Effect of growth temperature on the lipid composition of *Cyanidium caldarium*, Plant Physiol. 46 (1970) 290–293.
[4] M. Sinensky, Temperature control of phospholipid biosynthesis in *Escherichia coli*, J. Bacteriol. 106 (1971) 449–455.
[5] N.C. Johnston, H. Goldfine, Effects of growth temperature on fatty acid and alk-1-enyl group compositions of *Veillonella parvula* and *Megasphaera eksdenii* phospholipids, J. Bacteriol. 149 (1982) 567–575.
[6] E.F. DeLong, A.A. Yayanos, Adaptation of the membrane lipids of a deep-sea bacterium to changes in hydrostatic pressure, Science 228 (1985) 1101–1103.
[7] D. Bartlett, Pressure effects on in vivo microbial processes, Biochim. Biophys. Acta 1595 (2002) 367–381.
[8] M. Könneke, F. Widdel, Effect of growth temperature on cellular fatty acids in sulphate-reducing bacteria, Environ. Microbiol. 5 (2003) 1064–1070.
[9] A.R. Cossins, A.G. MacDonald, Homeoviscous theory under pressure II. The fatty acid composition of liver mitochondrial phospholipids of deep-sea fish, Biochim. Biophys. Acta 860 (1986) 325–335.
[10] S. Mabrey, J.M. Sturtevant, Investigation of phase transitions of lipids and lipid mixtures by high sensitivity differential scanning calorimetry, Proc. Natl. Acad. Sci. U.S.A. 73 (1976) 3862–3866.
[11] D.L. Melchior, J.M. Steim, Thermotropic transitions in biomembranes, Annu. Rev. Biophys. Bioeng. 5 (1976) 205–238.
[12] J.H. Ipsen, O. Karlström, O.G. Mouritsen, H. Winterström, M.J. Zuckermann, Phase equilibria in the phosphocholine–cholesterol system, Biochim. Biophys. Acta 905 (1987) 162–172.
[13] R. Koynova, M. Caffrey, Phases and phase transitions of the phosphocholines, Biochim. Biophys. Acta 1376 (1998) 91–145.
[14] T. Heimburg, A.D. Jackson, The thermodynamics of general anesthesia, Biophys. J. 92 (2007) 3159–3165.
[15] M. Sinensky, Homeoviscous adaptation-a homeostatic process the regulates the viscosity of membrane lipid in *Escherichia coli*, Proc. Natl. Acad. Sci. U.S.A. 71 (1974) 522–525.
[16] A.R. Cossins, A.G. MacDonald, Homeoviscous theory under pressure II. The molecular order of membranes from deep-sea fish, Biochim. Biophys. Acta 776 (1984) 144–150.
[17] A.G. Lee, Lipids and their effects on membrane proteins: evidence against a role for fluidity, Prog. Lipid Res. 30 (1991) 323–348.
[18] E. Sackmann, Biological membranes, Ch. Physical Basis of Trigger Processes and Membrane Structure, Academic Press, 1984, pp. 105–143.
[19] D. Brown, E. London, Functions of lipid rafts in biological membranes, ARCDB 14 (1998) 111–136.
[20] T. Heimburg, Mechanical aspects of membrane thermodynamics. Estimation of the mechanical properties of lipid membranes close to the chain melting transition from calorimetry, Biochim. Biophys. Acta 1415 (1998) 147–162.
[21] H. Ebel, P. Grabitz, T. Heimburg, Enthalpy and volume changes in lipid membranes. I. The proportionality of heat and volume changes in the lipid melting transition and its implication for the elastic constants, J. Phys. Chem., B 105 (2001) 7353–7360.
[22] M.F. Schneider, D. Marsh, W. Jahn, B. Kloesgen, T. Heimburg, Network formation of lipid membranes: triggering structural transitions by chain melting, Proc. Natl. Acad. Sci. U.S.A. 96 (1999) 14217–14312.
[23] J.F. Nagle, H. Scott, Lateral compressibility of lipid mono- and bilayers. Theory of membrane permeability, Biochim. Biophys. Acta 513 (1978) 236–243.
[24] T. Heimburg, A.D. Jackson, On soliton propagation in biomembranes and nerves, Proc. Natl. Acad. Sci. U.S.A. 102 (2005) 9790–9795.
[25] G.W. Feigenson, J.T. Buboltz, Ternary phase diagram of dipalmitoyl-pc/dilauroyl-pc/cholesterol: nanoscopic domain formation driven by cholesterol, Biophys. J. 80 (2001) 2775–2788.
[26] C. Leidy, W.F. Wolkers, K. Jorgensen, O.G. Mouritsen, J.H. Crowe, Lateral organization and domain formation in a two-component lipid membrane system, Biophys. J. 80 (2001) 1819–1828.
[27] J. Korlach, P. Schwille, W.W. Webb, G. Feigenson, Characterization of lipid bilayer phases by confocal microscopy and fluorescence correlation spectroscopy, Proc. Natl. Acad. Sci. U.S.A. 96 (1999) 8461–8466.
[28] L.A. Bagatolli, E. Gratton, Two-photon fluorescence microscopy observation of shape changes at the phase transition in phospholipid giant unilamellar vesicles, Biophys. J. 77 (1999) 2090–2101.
[29] M. Fidorra, L. Duelund, C. Leidy, A. Simonsen, L. Bagatolli, Absence of fluid-ordered/fluid-disordered phase coexistence in ceramide/POPE mixtures containing cholesterol, Biophys. J. 90 (2006) 4437–4451.
[30] D. Chapman, Liquid crystalline properties of phospholipids and biological membranes, Symp. Faraday Soc. 5 (1971) 163–174.
[31] E.C. Melo, I.M. Lourtie, M.B. Sankram, T.E. Thompson, Effects of domain connection and disconnection on the yields of in-plane bimolecular reactions in membranes, Biophys. J. 63 (1992) 1506–1512.
[32] T. Thompson, M. Sankram, R. Biltonen, D. Marsh, W. Vaz, Effects of domain structure on in-plane reactions and interactions, Mol. Membr. Biol. 12 (1995) 157–162.
[33] A. Hinderliter, R.L. Biltonen, P.F. Almeida, Lipid modulation of protein-induced membrane domains as a mechanism for controlling signal transduction, Biochemistry 43 (2004) 7102–7110.
[34] D.G. Salinas, M.D.L. Feunte, J.G. Reyes, Changes of enzyme activity in lipid signaling pathways related to substrate reordering, Biophys. J. 89 (2005) 885–894.
[35] J.A.F.O.D. Kamp, M.T. Kauerz, L.V. Deenen, Action of pancreatic phopsholipase A_2 on phosphatidylcholine bilayers in different physical states, Biochim. Biophys. Acta 406 (1975) 169–177.
[36] D. Lichtenberg, G. Romero, M. Menashe, R.L. Biltonen, Hydrolysis of dipalmytoyl-phosphatidylcholine large unilamellar vesicles by porcine pancreatic phospholipase A_2, J. Biol. Chem. 261 (1986) 5334–5340.
[37] D. Grainger, A. Reichert, H. Ringsdorf, C. Salesse, An enzyme caught in action: direct imaging of hydrolytic function and domain formation of phospholipase A_2 in phosphatidylcholine monolayers, FEBS Lett. 252 (1989) 73–82.
[38] C. Leidy, L. Linderoth, T.L. Andresen, O.G. Mouritsen, K. Jorgensen, Domain-induced activation of human phospholipase A_2 type IIA: local versus global lipid composition, Biophys. J. 90 (2006) 3165–3175.
[39] B. Cannon, M. Hermansson, S. Györke, P. Somerharju, J.A. Virtanen, K.H. Cheng, Regulation of calcium channel activity by lipid domain formation in planar lipid bilayers, Biophys. J. 85 (2003) 933–942.
[40] E.J. Bolen, J.J. Sando, Effect of phospholipid unsaturation on protein kinase C activation, Biochemistry 31 (1992) 5945–5951.
[41] A.R.G. Dibble, A.K. Hinderliter, J. Sando, R.L. Biltonen, Lipid lateral heterogeneity in phosphatidylcholine/phosphatidylserine/diacylglycerol vesicles and its influence on protein kinase C activation, Biophys. J. 71 (1996) 1877–1890.
[42] D. Tang, W.L. Dean, D. Borchman, C.A. Paterson, The influence of membrane lipid structure on plasma membrane Ca^{2+}-ATPase activity, Cell Calcium 39 (2006) 209–216.
[43] A.G. Lee, Lipid phase transitions and phase diagrams II. Mixtures involving lipids, Biochim. Biophys. Acta 472 (1977) 285–344.
[44] D. Guard-Friar, C.H. Chen, A.S. Engle, Deuterium isotope effect on the stability of molecules: phospholipids, J. Phys. Chem. 89 (1985) 1810–1813.
[45] G. Wang, C.H. Chen, Thermodynamic elucidation of structural stability of deuterated biological molecules: deuterated phospholipid vesicles in H_2O, Arch. Biochem. Biophys. 301 (1993) 330–335.
[46] S. Marcelja, Chain ordering in liquid crystals II. Structure of bilayer membranes, Biochim. Biophys. Acta 367 (1974) 165–176.
[47] D.A. Pink, T.J. Green, D. Chapman, Raman scattering in bilayers of saturated phosphatidylcholines. Experiment and theory, Biochemistry 19 (1980) 349–356.
[48] I.P. Sugar, T.E. Thompson, R.L. Biltonen, Monte Carlo simulation of two-component bilayers: DMPC/DSPC mixtures, Biophys. J. 76 (1999) 2099–2110.
[49] E.I. Michonova-Alexova, I.P. Sugar, Component and state separation in DMPC/DSPC lipid bilayers: a Monte Carlo simulation study, Biophys. J. 83 (2002) 1820–1833.
[50] H.M. Seeger, M. Fidorra, T. Heimburg, Domain size and fluctuations at domain interfaces in lipid mixtures, Macro. Symposia 219 (2005) 85–96.
[51] L. Cruzeiro-Hansson, O.G. Mouritsen, Passive ion permeability of lipid membranes modeled via lipid-domain interfacial area, Biochim. Biophys. Acta 944 (1988) 63–72.
[52] A.E. Hac, H.M. Seeger, M. Fidorra, T. Heimburg, Diffusion in two-component lipid membranes — a fluorescence correlation spectroscopy and Monte Carlo simulation study, Biophys. J. 88 (2005) 317–333.
[53] I. Sugar, R.L. Biltonen, Lateral diffusion of molecules in two-component lipid bilayer: a Monte Carlo simulation study, J. Phys. Chem. B 109 (2005) 7373–7386.
[54] L.K. Tamm, S.A. Tatulian, Infrared spectroscopy of proteins and peptides in lipid bilayers, Q. Rev. Biophys. 30 (1997) 365–429.
[55] R. Mendelsohn, G. Liang, H. Strauss, R. Snyder, IR spectroscopic determination of gel state miscibility in long-chain phosphatidylcholine mixtures, Biophys. J. 69 (1995) 1987–1998.
[56] H. Reinl, T. Brunn, T.M. Bayerl, Changes of the physical properties of the liquid-ordered phase with temperature in binary mixtures of DPPC with cholesterol, Biophys. J. 61 (1992) 1025–1035.
[57] H.M. Seeger, T. Heimburg, Relaxation processes in binary lipid mixtures: a Monte Carlo simulation study, in preparation.
[58] T. Heimburg, D. Marsh, Investigation of secondary and tertiary structural changes of cytochrome *c* in complexes with anionic lipids using amide hydrogen exchange measurements: An FTIR study, Biophys. J. 65 (1993) 2408–2417.
[59] T. Hill, Introduction to Statistical Thermodynamics, 2nd Edition, Addison-Wesley, 1962.
[60] I.P. Sugar, R.L. Biltonen, Structure-function relationships in two-component phospholipid bilayers. A Monte Carlo simulation approach using a two-state model, Methods Enzymol. 323 (2000) 340–372.
[61] S. Doniach, Thermodynamic fluctuations in phospholipid bilayer, J. Chem. Phys. 68 (1978) 4912–4916.
[62] S. Singer, G.L. Nicolson, The fluid mosaic model of the structure of cell membranes, Science 175 (1972) 720–731.
[63] K. Jacobson, E.D. Sheets, R. Simson, Revisiting the fluid mosaic model of membranes, Science 268 (1995) 1441–1442.
[64] B. Lagerholm, G.E. Weinreb, K. Jacobson, N.L. Thompson, Detecting microdomains in intact cell membranes, Annu. Rev. Phys. Chem. 56 (2005) 309–336.
[65] M. Fidorra, T. Heimburg, L. Bagatolli, Direct visualization of the lateral structure of cerebrosides/POPC mixtures in presence and absence of cholesterol. (submitted for publication).
[66] J.W. Orr, A.C. Newton, Interaction of protein kinase c with phosphatidylserine. 1. Cooperativity in lipid binding, Biochemistry 31 (1992) 4661–4667.